11

Turbulence in Stratified Fluids

Summary: Whereas the previous chapter treated organized wave flows in stratified fluids, the attention now turns to more complicated motions, such as vertical mixing, flow instability, forced turbulence, and convection. Because the investigation of such phenomena does not lend itself to detailed mathematical treatment, the emphasis is on budgets and scale analysis. The all-important Richardson number is introduced and discussed.

11-1 MIXING OF STRATIFIED FLUIDS

Mixing by turbulence generates vertical motions and overturning. In a homogeneous fluid, the supply of energy is only that necessary to overcome mechanical friction. But, in a stratified fluid, work must be performed to raise heavy fluid parcels and lower light parcels. Let us consider, for example, the system pictured in Figure 11-1. Initially, it consists of two layers of equal thicknesses with fluids of different densities and horizontal velocities. After some time, mixing is assumed to have taken place, and the system consists of a single layer of average density flowing with the average velocity.[1]

[1] Credit for this illustrative example goes to Prof. William K. Dewar.

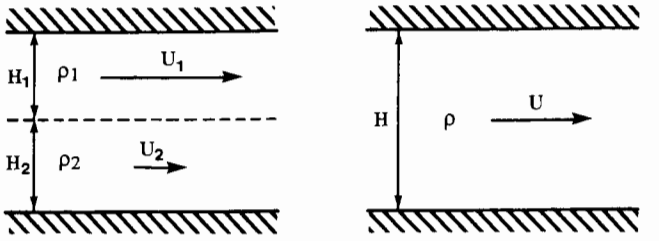

Initial State (prior to mixing)

Final State (after complete mixing)

Figure 11-1 Mixing of a two-layer stratified fluid with velocity shear. Rising of dense fluid and downwelling of light fluid requires work against buoyancy forces and thus leads to an increase in potential energy. Concomitantly, the kinetic energy of the system decreases during mixing. Only when the kinetic-energy drop exceeds the potential-energy rise can mixing proceed spontaneously.

Because initially the heavier fluid (density ρ_2) lies below the lighter fluid (density ρ_1), the center of gravity falls below middepth level, whereas in the final state it is exactly at middepth. Thus, the center of gravity has been raised in the mixing process, and potential energy must have been provided to the system. With identical initial depths $H_1 = H_2 = H/2$, the average density is $\rho = (\rho_1 + \rho_2)/2$, and the potential energy gain is

$$\begin{aligned} PE \text{ gain} &= \int_0^H \rho_{\text{final}}\, gz\, dz - \int_0^H \rho_{\text{initial}}\, gz\, dz \\ &= \frac{1}{2}\,\rho g H^2 - \left[\frac{1}{2}\,\rho_2 g\,\frac{H^2}{4} + \frac{1}{2}\,\rho_1 g\,\frac{3H^2}{4}\right] \\ &= \frac{1}{8}\,(\rho_2 - \rho_1) g H^2 . \end{aligned} \tag{11-1}$$

The question arises as to the source of this energy increase. Because human intervention is ruled out in geophysical flows, a natural energy supply must exist or mixing would not take place. It turns out that kinetic energy is released in the process, provided that the initial velocity distribution is uneven. Conservation of linear momentum in the absence of external forces implies that the final, uniform velocity is the average of the initial velocities of each layer: $U = (U_1 + U_2)/2$, thus leading to a kinetic-energy loss:

$$\begin{aligned} KE \text{ loss} &= \int_0^H \frac{1}{2}\,\rho_0\, u^2_{\text{initial}}\, dz - \int_0^H \frac{1}{2}\,\rho_0\, u^2_{\text{final}}\, dz \\ &= \frac{1}{2}\,\rho_0 U_2^2 \frac{H}{2} + \frac{1}{2}\,\rho_0 U_1^2 \frac{H}{2} - \frac{1}{2}\rho_0 U^2 H \\ &= \frac{1}{8}\,\rho_0 (U_1 - U_2)^2 H. \end{aligned} \tag{11-2}$$

Here, we have invoked the Boussinesq approximation: $\rho_1 \simeq \rho_2 \simeq \rho_0$.

Complete vertical mixing is naturally possible as long as the kinetic-energy loss exceeds the potential-energy gain; that is,

$$\frac{(\rho_2 - \rho_1)gH}{\rho_0 (U_1 - U_2)^2} < 1 . \tag{11-3}$$

Physically, the initial density difference should be sufficiently weak in order not to present an insurmountable gravitational barrier, or the initial velocity shear should be sufficiently large to supply the necessary amount of energy. When criterion (11-3) is not met, mixing occurs only in the vicinity of the initial interface and cannot extend over the entire system. The determination of the characteristics of such localized mixing calls for a more detailed analysis.

For this purpose, let us now consider a two-fluid system of infinite extent (Figure 11-2a), with upper and lower densities and velocities denoted, respectively, by ρ_1, ρ_2 and U_1, U_2, and let us explore interfacial waves of infinitesimal amplitudes. Mathemat-

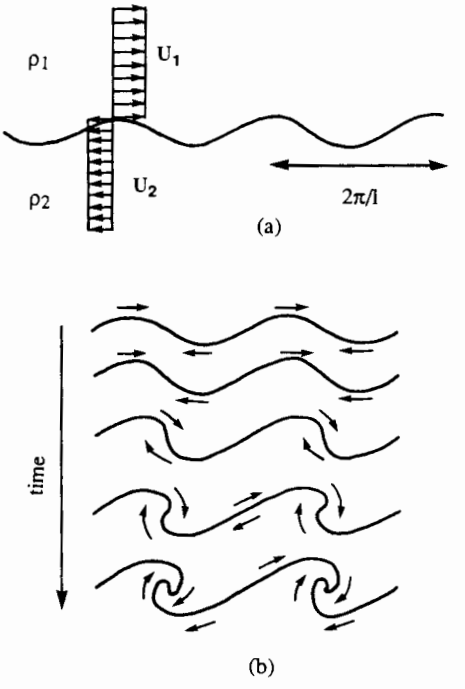

Figure 11-2 Kelvin–Helmholtz instability: (a) initial perturbation of wave number l, (b) time evolution of an unstable perturbation. The system is always unstable to short waves, which steepen, overturn, and eventually cause mixing. As waves overturn, their vertical and lateral extents are of comparable magnitudes.

ical derivations, not reproduced here, show that a sinusoidal perturbation of wave number l (wavelength $2\pi/l$) is unstable if (Kundu, 1990, Section 11-6)

$$(\rho_2^2 - \rho_1^2)g < \rho_1 \rho_2 l \, (U_1 - U_2)^2 ,$$

or for a Boussinesq fluid ($\rho_1 \simeq \rho_2 \simeq \rho_0$),

$$2(\rho_2 - \rho_1)g < \rho_0 l \, (U_1 - U_2)^2 . \tag{11-4}$$

In a stability analysis, waves of all wavelengths must be considered, and we conclude that there will always be sufficiently short waves to cause instabilities. Therefore, a

two-layer shear flow is always unstable. This is known as the *Kelvin–Helmholtz instability*. Incidentally, this instability explains the generation of water waves by surface winds.

The details of the analysis leading to (11-4) reveal that the interfacial waves induce flow perturbations that extend on both sides of the interface over a depth on the order of their wavelength. Thus, as unstable waves grow, they form rolls of depth comparable to their width (Figure 11-2b; Figure 11-3).

The rolling and breaking of waves induces turbulent mixing; naturally, the vertical extent of the mixing zone, which we will denote by ΔH, is proportional to the wavelength of the longest unstable wave, that for which criterion (11-4) turns into an equality:

$$\Delta H \simeq \frac{1}{l_{\min}} = \frac{\rho_0 (U_1 - U_2)^2}{2(\rho_2 - \rho_1) g}. \tag{11-5}$$

If the fluid system is of finite depth H, the preceding theory is no longer applicable, but we can anticipate, by virtue of dimensional analysis, that the results still hold, within some numerical factors. For a fluid depth H greater than ΔH, mixing must remain localized to a band of thickness ΔH, whereas for a fluid depth H less than ΔH, that is,

$$H \lesssim \frac{\rho_0 (U_1 - U_2)^2}{(\rho_2 - \rho_1) g}, \tag{11-6}$$

mixing will engulf the entire system. Note the similarity between this last inequality, derived from a wave theory, and inequality (11-3), obtained from energy considerations.

11-2 INSTABILITY OF A STRATIFIED SHEAR FLOW

In the preceding section, we restricted our considerations to a finite discontinuity of the horizontal velocity, only to find that such a discontinuity is always unstable. Instability causes mixing, and mixing will proceed until the velocity profile has been made stable. The question then is: For a given density stratification, what is the critical velocity shear below which the system is stable and above which mixing occurs? To answer this question, we are led to study the stability of a stratified shear flow.

Let us consider a two-dimensional (x, z) inviscid and nondiffusive fluid with horizontal and vertical velocities (u, w), dynamic pressure p, and density anomaly ρ. In anticipation of the important role played by vertical motions, we reinstate the acceleration term in the vertical momentum equation and write (Section 3-5)

$$\frac{\partial u}{\partial t} + u \frac{\partial u}{\partial x} + w \frac{\partial u}{\partial z} = -\frac{1}{\rho_0} \frac{\partial p}{\partial x} \tag{11-7a}$$

$$\frac{\partial w}{\partial t} + u \frac{\partial w}{\partial x} + w \frac{\partial w}{\partial z} = -\frac{1}{\rho_0} \frac{\partial p}{\partial z} - \frac{\rho g}{\rho_0} \tag{11-7b}$$

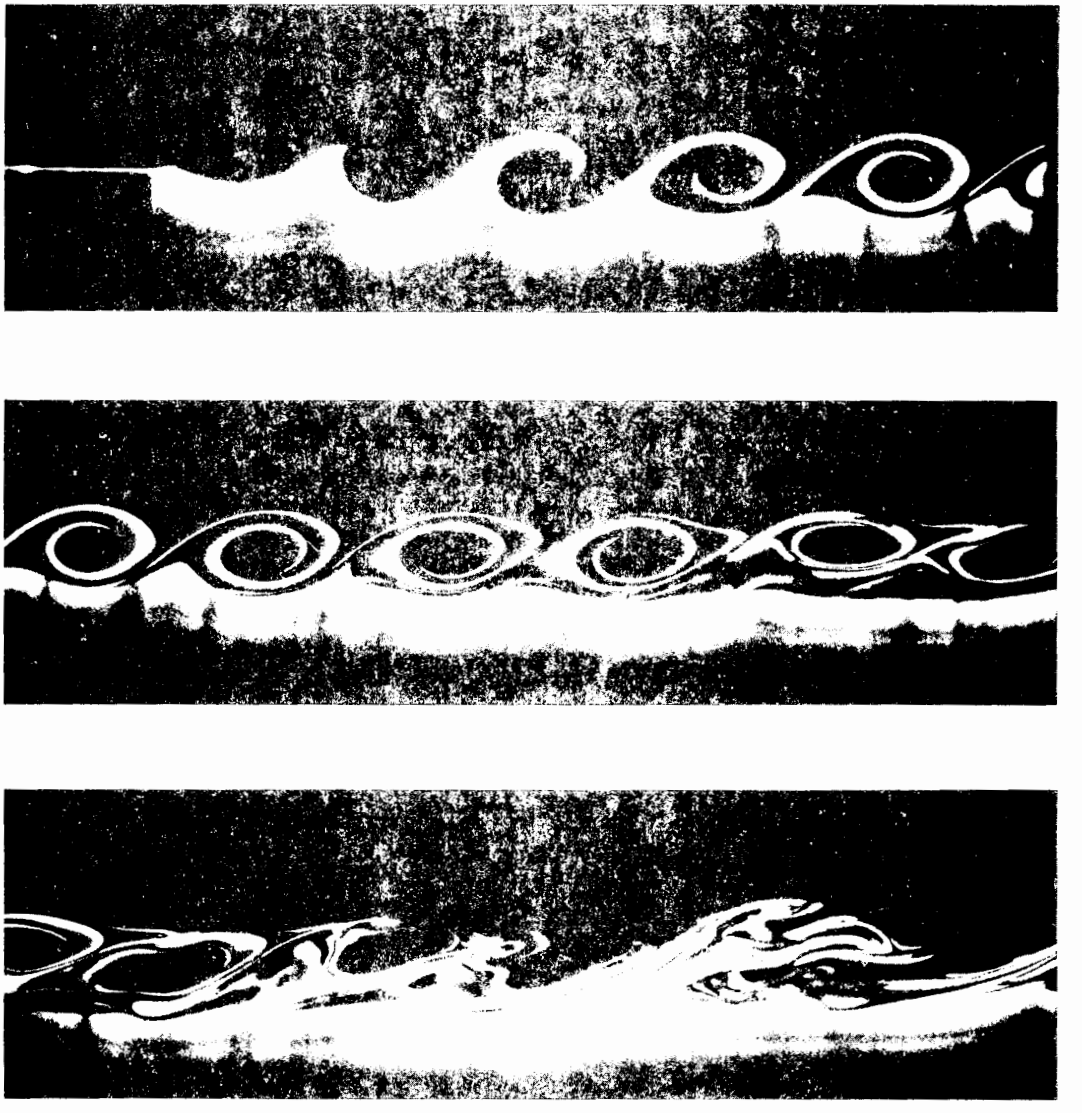

Figure 11-3 Development of a Kelvin–Helmoholtz instability in the laboratory. Here, two layers flowing from left to right join downstream of a thin plate (visible on the left of the top photograph). The upper and faster moving layer is slightly less dense than the lower layer. Downstream distance (from left to right on each photograph and from top to bottom panel) plays the role of time. At first, waves form and overturn in a two-dimensional fashion but, later, three-dimensional motions appear and lead to turbulence and mixing. (Courtesy of Greg A. Lawrence. For more details on the laboratory experiment, see Lawrence et al., 1991.)

$$\frac{\partial u}{\partial x} + \frac{\partial w}{\partial z} = 0 \tag{11-7c}$$

$$\frac{\partial \rho}{\partial t} + u \frac{\partial \rho}{\partial x} + w \frac{\partial \rho}{\partial z} = 0. \tag{11-7d}$$

Our basic state consists of a steady, sheared horizontal flow [$u = \bar{u}(z)$, $w = 0$] in a vertical density profile [$\rho = \bar{\rho}(z)$]. The accompanying pressure field $\bar{p}(z)$ obeys $d\bar{p}/dz = -g\bar{\rho}(z)$. The addition of an infinitesimally small perturbation ($u = \bar{u} + u'$, $w = w'$, $p = \bar{p} + p'$, $\rho = \bar{\rho} + \rho'$) and a subsequent linearization of the equations yield:

$$\frac{\partial u'}{\partial t} + \bar{u} \frac{\partial u'}{\partial x} + w' \frac{d\bar{u}}{dz} = -\frac{1}{\rho_0} \frac{\partial p'}{\partial x} \tag{11-8a}$$

$$\frac{\partial w'}{\partial t} + \bar{u} \frac{\partial w'}{\partial x} = -\frac{1}{\rho_0} \frac{\partial p'}{\partial z} - \frac{\rho' g}{\rho_0} \tag{11-8b}$$

$$\frac{\partial u'}{\partial x} + \frac{\partial w'}{\partial z} = 0 \tag{11-8c}$$

$$\frac{\partial \rho'}{\partial t} + \bar{u} \frac{\partial \rho'}{\partial x} + w' \frac{d\bar{\rho}}{dz} = 0. \tag{11-8d}$$

Introducing the perturbation streamfunction ψ via $u' = +\partial\psi/\partial z$, $w' = -\partial\psi/\partial x$, the buoyancy frequency $N^2 = -(g/\rho_0)(d\bar{\rho}/dz)$, assumed to be constant, and a Fourier structure $\exp[il(x - ct)]$ in the horizontal, we can reduce the problem to a single equation for ψ in terms of the remaining variable, z:

$$(\bar{u} - c)\left(\frac{d^2\psi}{dz^2} - l^2\psi\right) + \left(\frac{N^2}{\bar{u} - c} - \frac{d^2\bar{u}}{dz^2}\right)\psi = 0. \tag{11-9}$$

This is the *Taylor–Goldstein equation*. It governs the vertical structure of a perturbation in a stratified parallel flow. Note the formal analogy with the Rayleigh equation (7-12) governing the structure of a perturbation on a horizontally sheared flow in the absence of stratification and in the presence of rotation. Therefore, the same analysis can be applied.

First, we state our boundary conditions. If we consider our domain to be bounded vertically by two horizontal planes, at $z = 0$ and H, we impose a zero vertical velocity there, or, in terms of the streamfunction:

$$\psi(0) = \psi(H) = 0. \tag{11-10}$$

Then, we recognize that the equation and its accompanying boundary conditions form an eigenvalue problem: Unless the phase velocity c takes on a particular value (eigenvalue), the solution is trivial ($\psi = 0$). In general, the eigenvalues may be complex, but if c admits the function ψ, then its complex conjugate c^* admits the function ψ^* and is thus another eigenvalue. This can be easily verified by taking the complex conjugates of (11-9) and (11-10). Hence, complex eigenvalues come in pairs. In each pair, one of

the two eigenvalues will have a positive imaginary part and will correspond to an exponentially growing perturbation. The presence of a nonzero imaginary part to c automatically guarantees the existence of at least one unstable mode. Conversely, the basic flow is stable if and only if all possible phase speeds c are purely real.

Because it is impossible to solve problems (11-9) and (11-10) in the general case of an arbitrary shear flow $\bar{u}(z)$, we will content ourselves, as in Section 7-2, to derive integral constraints. A variety of such constraints can be established, but the most powerful one is obtained when the function ϕ, defined by

$$\psi = \sqrt{\bar{u} - c}\ \phi, \tag{11-11}$$

is used to replace ψ. Equation (11-9) and boundary conditions (11-10) become

$$\frac{d}{dz}\left[(\bar{u} - c)\frac{d\phi}{dz}\right] - \left[l^2(\bar{u} - c) + \frac{1}{2}\frac{d^2\bar{u}}{dz^2} + \frac{1}{\bar{u} - c}\left(\frac{1}{4}\left(\frac{d\bar{u}}{dz}\right)^2 - N^2\right)\right]\phi = 0, \tag{11-12}$$

$$\phi(0) = \phi(H) = 0. \tag{11-13}$$

Multiplying equation (11-12) by the complex conjugate ϕ^*, integrating over the vertical extent of the domain, and utilizing conditions (11-13), we obtain

$$\int_0^H \left[N^2 - \frac{1}{4}\left(\frac{d\bar{u}}{dz}\right)^2\right]\frac{|\phi|^2}{\bar{u} - c}\,dz = \int_0^H (\bar{u} - c)\left(\left|\frac{d\phi}{dz}\right|^2 + l^2|\phi|^2\right)dz + \frac{1}{2}\int_0^H \frac{d^2\bar{u}}{dz^2}\,|\phi|^2\,dz, \tag{11-14}$$

where vertical bars denote the absolute value of complex quantities. The imaginary part of this expression is

$$c_i \int_0^H \left[N^2 - \frac{1}{4}\left(\frac{d\bar{u}}{dz}\right)^2\right]\frac{|\phi|^2}{|\bar{u} - c|^2}\,dz = -c_i \int_0^H \left(\left|\frac{d\phi}{dz}\right|^2 + l^2|\phi|^2\right)dz,$$

where c_i is the imaginary part of c. If the flow is such that $N^2 > \frac{1}{4}(d\bar{u}/dz)^2$ everywhere, then the preceding equality requires that c_i times a positive quantity equals c_i times a negative quantity and, consequently, that c_i can only be zero. Defining the *Richardson number*

$$Ri = \frac{N^2}{(d\bar{u}/dz)^2}, \tag{11-15}$$

we can state that if the inequality

$$Ri > \frac{1}{4} \tag{11-16}$$

holds everywhere in the domain, the stratified shear flow is stable. Note that the

criterion does not imply that c_i must be nonzero if the Richardson number falls below $\frac{1}{4}$ somewhere in the domain. Hence, inequality (11-16) is a sufficient condition for stability, while its converse is a necessary condition for instability. Atmospheric, oceanic, and laboratory data reveal, however, that the converse of (11-16) is generally a reliable predictor of instability.

If the shear flow is characterized by linear variations of velocity and density (note that a linear density variation was already implicitly assumed when we required N^2 to be constant), with velocities and densities ranging from U_1 to U_2 and ρ_1 to ρ_2 ($\rho_2 > \rho_1$), respectively, over a depth H, then

$$\frac{d\bar{u}}{dz} = \frac{U_1 - U_2}{H}, \qquad N^2 = \frac{g}{\rho_0}\frac{\rho_2 - \rho_1}{H},$$

and the Richardson criterion stated as the necessary condition for instability becomes opaque:

$$\frac{(\rho_2 - \rho_1)gH}{\rho_0 (U_1 - U_2)^2} < \frac{1}{4}. \tag{11-17}$$

The similarity to (11-3) is not coincidental: Both conditions imply the possibility of large perturbations that could destroy the stratified shear flow. The difference in the numerical coefficients on the right-hand sides can be explained by the difference in the choice of the basic profile [discontinuous for (11-3), linear for (11-17)] and by the fact that the analysis leading to (11-3) did not make provision for a consumption of kinetic energy by vertical motions. More importantly, the similarity between (11-3) and (11-17) imparts a physical meaning to the Richardson number: It is essentially a ratio between potential and kinetic energies, the numerator being the potential-energy barrier that mixing, if it is to occur, must overcome and the denominator being the kinetic energy in the shear flow available under the smoothing action of mixing. In fact, it was precisely by developing such energy considerations that British meteorologist Lewis Fry Richardson first arrived, in 1920, to the dimensionless ratio that now rightfully bears his name. A first formal proof of criterion (11-16), however, did not come until four decades later (Miles, 1961).

In closing this section, it may be worth mentioning for the record that bounds on the real and imaginary parts of the wave velocity c can be derived by the inspection of certain integrals. This analysis, due to American mathematician Louis N. Horward, has already been applied to the study of barotropic instability (Section 7-3). Here, we summarize Howard's original derivation in the context of stratified shear flow. To begin, we introduce the vertical displacement a caused by the small perturbation

$$\frac{\partial a}{\partial t} + \bar{u}\frac{\partial a}{\partial x} = w$$

or

$$(\bar{u} - c)a = -\psi.$$

We then eliminate ψ from (11-9) and (11-10) and obtain an equivalent problem for the variable a:

$$\frac{d}{dz}\left[(\bar{u}-c)^2\,\frac{da}{dz}\right]+\left[N^2-l^2(\bar{u}-c)^2\right]a=0, \tag{11-18a}$$

$$a(0)=a(H)=0. \tag{11-18b}$$

A multiplication by the complex conjugate a^* followed by an integration over the domain and use of the boundary conditions yields

$$\int_0^H (\bar{u}-c)^2 P\,dz=\int_0^H N^2|a|^2\,dz, \tag{11-19}$$

where $P=|da/dz|^2+l^2|a|^2$ is a nonzero positive quantity. The imaginary part of this equation implies that if there is instability ($c_i\neq 0$), c_r must lie between the minimum and maximum values of $\bar{u}$, that is,

$$U_{\min}<c_r<U_{\max}. \tag{11-20}$$

Physically, the growing perturbation travels with the flow at some intermediate speed, and there exists at least one critical level in the domain where the perturbation is stationary with respect to the local flow. This local coupling between the wave and the flow is precisely what allows the wave to extract energy from the flow and to grow at its expense.

Now, the real part of (11-19),

$$\int_0^H |(\bar{u}-c_r)^2-c_i^2|P\,dz=\int_0^H N^2|a|^2\,dz \tag{11-21}$$

can be manipulated in a way similar to that used in Section 7-3 to obtain the following inequality:

$$\left(c_r-\frac{U_{\min}+U_{\max}}{2}\right)^2+c_i^2\leq\left(\frac{U_{\max}-U_{\min}}{2}\right)^2. \tag{11-22}$$

This implies that, in the complex plane, the number $c=c_r+ic_i$ must lie within the circle that has the range $\bar{u}$ as diameter on the real axis. Because instability requires a positive imaginary value c_i, the interest is restricted to the upper half of the circle (Figure 7-1). This result is called the Howard semicircle theorem. In particular, it implies that c_i is bounded by $(U_{\max}-U_{\min})/2$, providing a useful upper bound on the growth rate of unstable perturbations:

$$lc_i\leq\frac{l}{2}(U_{\max}-U_{\min}). \tag{11-23}$$

11-3 TURBULENCE IN A STRATIFIED SHEAR FLOW

Like mixing, turbulence in stratified fluids requires work against buoyancy forces, and stratification thus acts as a moderator of turbulence. This situation can be expressed quantitatively by applying to turbulence some of the concepts derived earlier, particularly the notion of mixing depth, as expressed by (11-5),

$$\Delta H = \frac{\rho_0 \ (U_1 - U_2)^2}{2g \ (\rho_2 - \rho_1)}, \tag{11-24}$$

can be adapted as follows. An important measure of turbulence is the *friction velocity* u_*, a measure of the turbulent velocity fluctuations. (The attribute *friction* reflects the historical heritage of turbulent boundary-layer theory and does not imply that friction is of great importance here.) Thus, locally horizontal velocities are expected to differ by values on the order of u_*, and the numerator of (11-24) could be replaced by the dimensionally equivalent expression $\rho_0 u_*^2$. Likewise, the difference $(\rho_2 - \rho_1)$ can be interpreted as a local turbulent density fluctuation and the product $u_* \ (\rho_2 - \rho_1)$, as a measure of the vertical density flux $\overline{w'\rho'}$ (where primes denote turbulent fluctuations and an overbar indicates some average). The introduction of those quantities transforms (11-24) into a turbulent analogue:

$$L = \frac{\rho_0 \ u_*^3}{\kappa g \ \overline{w'\rho'}}. \tag{11-25}$$

This length scale represents the depth of fluid to which stratification confines eddies of strength u_*. It is called the *Monin–Obukhov length* in honor of the two Soviet oceanographers who, in 1954, first pointed to the importance of this scale in the study of stratified turbulence. In the denominator, the factor κ is the von Karman constant ($\kappa = 0.40$), which is traditionally introduced to facilitate mathematical development in boundary-layer applications.

If density variations are entirely due to temperature stratification, then the flux $\overline{w'\rho'}$ is equal to $-\alpha\rho_0 \ \overline{w'T'}$, where α is the coefficient of thermal expansion and T' is the temperature fluctuation. Because this is generally the case, the Monin–Obukhov length is customarily defined as

$$L = \frac{u_*^3}{-\kappa\alpha g \overline{w'T'}}. \tag{11-26}$$

As an application, consider the development of a turbulent mixed layer in the upper ocean under the action of a wind stress (Figure 11-4). Let us assume that, initially, the ocean stratification is characterized by a uniform stratification frequency N, so that the density increases linearly with depth according to

$$\rho = -\frac{\rho_0 N^2}{g} \ z, \tag{11-27}$$

where z is the vertical coordinate measured negatively downward ($z = 0$ is the surface)

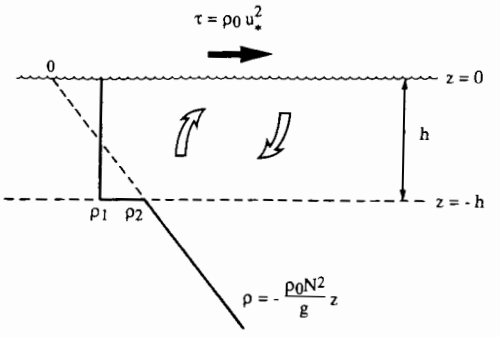

Figure 11-4 Development of a mixed layer in the ocean under the action of a wind stress.

and ρ is the density departure from the reference density ρ_0, the initial surface density. After some time t, this stratification has been partially eroded, and a mixed layer of depth h has developed. In this layer, the density has been homogenized and, in the absence of surface heating, evaporation, and precipitation, has become the average density that initially existed over that depth:

$$\rho_1 = \frac{\rho_0 N^2 h}{2g}.$$

Below the base of this mixed layer, the density is still unchanged, $\rho_2 = \rho(z = -h) = \rho_0 N^2 h/g$, and there is thus a density jump

$$\Delta\rho = \rho_2 - \rho_1 = \frac{\rho_0 N^2 h}{2g}. \tag{11-28}$$

Mixing has caused upwelling of denser waters and downwelling of lighter waters, thus raising the level of potential energy. The energy gain by time t is

$$PE = \int_{-h}^{H} \rho_1 g z \, dz - \int_{-h}^{H} \rho g z \, dz$$

$$= \frac{1}{12} \rho_0 N^2 h^3 .$$

Therefore, potential energy increases at the rate

$$\frac{dPE}{dt} = \frac{1}{4} \rho_0 N^2 h^2 \frac{dh}{dt}. \tag{11-29}$$

The supply of energy is provided by the surface wind. If the wind stress is τ, the turbulent friction velocity u_* is given by (Kundu, 1990, Section 12-11)

$$\tau = \rho_0 u_*^2, \tag{11-30}$$

and the rate of work performed by τ on fluid particles with typical velocities u_* is proportional to τu_* or $\rho_0 u_*^3$. Introducing a coefficient of proportionality m to account

for the exact rate of work minus the portion diverted to kinetic-energy production, we state: $dPE/dt = m\rho_0 u_*^3$, or by virtue of (11-29),

$$N^2 h^2 \frac{dh}{dt} = 4mu_*^3 . \tag{11-31}$$

Observations and laboratory experiments suggest $m = 1.25$. This equation can be readily integrated to obtain the instantaneous mixed-layer depth:

$$h = \left(\frac{12mu_*^3}{N^2} t \right)^{1/3} . \tag{11-32}$$

Of some interest here is the evaluation of the Monin–Obukhov length. As the layer erodes the underlying stratification at the rate dh/dt, turbulence must overcome the density jump $\Delta\rho$, causing a density flux at the base of the mixed layer of magnitude

$$\overline{w'\rho'} = \frac{dh}{dt} \Delta\rho = \frac{2m\rho_0 u_*^3}{gh} ,$$

by virtue of (11-28) and (11-31). Based on this local flux value, the Monin–Obukhov length (11-25) is found to be

$$L = \frac{1}{2m\kappa} h . \tag{11-33}$$

With the numerical values $\kappa = 0.40$ and $m = 1.25$, L is exactly h. The exact identity between L and h is fortuitous, but it remains that the depth of the turbulent mixed layer is on the order of the Monin–Obukhov length, thus imparting a direct physical meaning to the latter.

The preceding considerations illustrate but one aspect of the development of a mixed layer in the upper ocean. Much work has been done on this problem, and the reader desiring additional information is referred to the book edited by Kraus (1977) for a review and to the article by Pollard et al. (1973) for a particularly clear discussion of Coriolis effects and of the relevance of the Richardson number. Considerations of mechanically induced mixing in the lower atmosphere and above the ocean floor can be found, respectively, in Sorbjan (1989, Section 4.4.1) and in Weatherly and Martin (1978). A review of laboratory experiments and associated theories is provided by Fernando (1991).

11-4 CONVECTION

Convection is defined as the process by which vertical motions modify the heat distribution in the system. In the example at the end of the previous section, the stirring of the upper ocean layer is caused by the mechanical action of the wind stress, and

convection is said to be forced. Natural, or free, convection arises when the only source of energy is of thermal origin, such as an imposed temperature difference or an imposed heat flux, and the motions associated with the convective process derive their energy from the work generated by buoyancy forces as warm fluid rises and cold fluid sinks.

A common occurrence of natural convection in geophysical fluids is the development of an unstable atmospheric boundary layer (Sorbjan, 1989). During daytime, the solar radiation traverses the atmosphere and reaches the earth (ground or sea), where it is absorbed. The earth reemits this radiation in the infrared range, thus effectively heating the atmosphere from below. As a result, the lowest level of the atmosphere is usually an unstable, convective region, called the *atmospheric boundary layer*. The existence of this layer is very beneficial to humans because of the ventilation it causes. When the atmosphere is stably stratified down to the ground, a phenomenon called *inversion*, the air is still and uncomfortable; moreover, if there is a source of pollution, this pollution stagnates and can become harmful. Such is the situation in Los Angeles (USA) when smog occurs (Stern et al., 1984).

The intensity of stirring motions in natural convection depends, obviously, on the strength of the thermal forcing as well as on the resistance of the fluid to move (viscosity) and to conduct heat (conductivity). A traditional example is convection in a fluid layer of height h confined between two horizontal rigid plates and heated from below. The forcing is the temperature difference ΔT between the two plates, the lower one being the hotter of the two. At low temperature differences, the viscosity ν and the heat diffusivity κ_T of the fluid prevent convective motions, the fluid remains at rest, and the heat is carried solely by molecular diffusion (conduction). As the temperature difference is increased, everything else remaining unchanged, the hot fluid at the bottom will eventually float upward and the cold fluid will sink from above.

If viscosity is the limiting factor, the amplitude of the convective velocities, w_*, can be estimated from a balance between the upward buoyancy force $-g\rho'/\rho_0 \sim \alpha g \Delta T$ (where α is the coefficient of thermal expansion) and the retarding frictional force $\nu \partial^2 w/\partial z^2 \sim \nu w_*/h^2$, yielding

$$w_* \sim \frac{\alpha g \Delta T h^2}{\nu}. \tag{11-34}$$

Comparing the convective heat flux $\overline{w'T'} \sim w_* \Delta T \sim \alpha g \Delta T^2 h^2/\nu$ to the conductive flux $\kappa_T \partial T/\partial z \sim \kappa_T \Delta T/h$, we form the ratio

$$Ra = \frac{\alpha g \Delta T^2 h^2/\nu}{\kappa_T \Delta T/h} = \frac{\alpha g \Delta T h^3}{\nu \kappa_T}, \tag{11-35}$$

which is known as the *Rayleigh number*, in honor of British scientist Lord Rayleigh, who first studied this problem quantitatively (1916). (Rayleigh was a contemporary of Kelvin; see the joint photograph at end of Chapter 6.)

Convection occurs, theories show (Chandrasekhar, 1961), when this number exceeds a critical value, which depends on the nature of the boundary conditions. For a fluid confined between two rigid plates, the critical Rayleigh number is $Ra = 1708$. At

values slightly above the threshold, convection organizes itself in parallel two-dimensional rolls or in packed hexagonal cells. At higher values of the Rayleigh number, erratic time-dependent motions develop, and convection appears much less organized.

Geophysical fluids almost always fall in this last category because of the large depths involved and the small values of molecular viscosity and conductivity of air and water. In the atmospheric boundary layer, where the Rayleigh number typically exceeds 10^{15}, convection is manifested by the intermittent formation near the ground of warm pockets of air, called *thermals*, which then rise through the convective layer; the circuit is completed by a weak subsidence of colder air between the rising thermals. In such a situation, viscosity and heat diffusivity play secondary roles, and the main characteristics of the flow do not depend on them.

As an application, consider the development of an atmospheric boundary layer from an initial, stable stratification under the action of a constant heat flux supplied by the ground (Figure 11-5). At time $t = 0$, the air is assumed linearly stratified with potential-temperature profile given by

$$\overline{T}(z) = T_0 + \Gamma z, \tag{11-36}$$

where T_0 is the initial potential temperature at the ground and Γ is the vertical potential-temperature gradient [corresponding to a stratification frequency $N = (\alpha g \Gamma)^{1/2}$]. The upward heat flux at the ground, denoted by $\rho_0 C_p Q$, is assumed constant. After some time t, convection has eroded the stratification up to a height h. The temperature T in the convective layer varies according to the instantaneous distribution

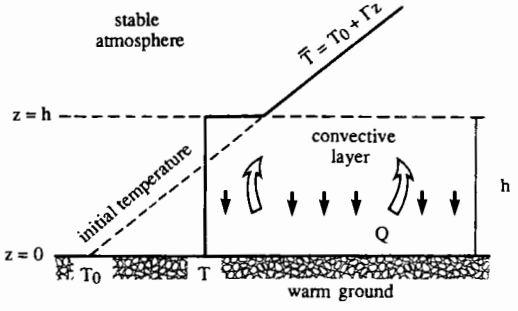

Figure 11-5 An unstable atmospheric boundary layer. The heat supplied at the surface generates convection, which progressively erodes the stratification.

of thermals but, on the average, appears to be nearly constant with height. The heat budget for the intervening time requires that the change in heat content of the affected fluid be equal to the accumulated heat received from the ground,

$$\rho_0 C_p \int_0^h (T - \overline{T})\, dz = \int_0^t \rho_0 C_p Q\, dt,$$

and provides a first relation between the height of the convective layer and its temperature:

$$h\,(T - T_0) - \tfrac{1}{2}\Gamma h^2 = Qt. \tag{11-37}$$

Another relation between these two variables arises from the mechanical-energy budget. Because there is no source of mechanical energy, the sum of the kinetic and potential energies of the system decays with time under the action of frictional forces. In first approximation, to be verified a posteriori, the amount of kinetic energy and energy loss to friction are insignificant contributions compared to the potential-energy changes undergone by the system. So, it suffices to state in first approximation that potential energy, per unit area, at time t is equal to that at the initial time:

$$\int_0^h \rho_0 \alpha T g z \, dz = \int_0^h \rho_0 \alpha \overline{T} g z \, dz,$$

which yields

$$T - T_0 = \tfrac{2}{3} \Gamma h. \tag{11-38}$$

Physically, this implies that the temperature rise at the ground is two-thirds of the temperature change over the height h according to the initial temperature gradient (Figure 11-5). Oddly enough, the temperature in the upper third of the convective layer is decreased, while the fluid undergoes an overall heating.

Together, equations (11-37) and (11-38) provide the temporal evolution of the thickness and potential temperature of the atmospheric boundary layer:

$$h = \sqrt{\frac{6Qt}{\Gamma}} \tag{11-39a}$$

$$T = T_0 + \sqrt{\frac{8\Gamma Qt}{3}}. \tag{11-39b}$$

The atmospheric boundary layer thus grows according to the square root of time. This progressive erosion of the ambient stratification by convective motions is termed *penetrative convection.*

We are now in a position to estimate the contribution of kinetic energy. Because convection is accomplished by thermals that rise over the entire extent of the layer, the convective overturns are as deep as the layer itself, and the Monin–Obukhov length is comparable to the layer thickness. Equating these two quantities, we write:

$$\frac{w_*^3}{\kappa \alpha g Q} = h,$$

where the symbol w_* replaces u_* to indicate that the turbulent motions are not mechanically induced (such as by a shear stress) but are of thermal origin. This equality yields a measure of the turbulent velocity w_*:

$$w_* = (\kappa \alpha g h Q)^{1/3}, \tag{11-40}$$

which supersedes (11-34) when the Rayleigh number is so high that viscosity is no

longer the dominant parameter. The kinetic energy is then estimated to be $\frac{1}{2}\rho_0 w_*^2 h$, and its ratio to the instantaneous potential energy $\frac{1}{2}\rho_0 \alpha g(T - T_0)h^2$ is

$$\frac{KE}{PE} \sim (Nt)^{-2/3}, \tag{11-41}$$

the numerical coefficients being discarded. In this last expression, $N = (\alpha g \Gamma)^{1/2}$ is the frequency of the undisturbed stratification. Because $1/N$ is typically on the order of a few minutes while the atmospheric boundary layer develops over hours, the product Nt is large, and we can justify our earlier neglect of the kinetic-energy contribution to the overall energy budget. A fortiori, the decay rate of kinetic energy by frictional forces is also unimportant in the overall energy budget. Finally, it is worth noting that if w_* is the velocity scale of the rising thermals, the heat flux $Q = \overline{w'T'}$ is carried by those thermals if their temperature differs from that of the descending fluid approximately by $T_* = Q/w_*$.

The preceding application is but a simple example of convection in the atmosphere. Generally, convective motions in the atmospheric boundary are affected by numerous factors, including winds, which they in turn affect. A sizable body of knowledge has been accumulated on the physics of the atmospheric boundary layer, and the interested reader is referred to Sorbjan (1989).

PROBLEMS

11-1. A stratified shear flow consists of two layers of depth H_1 and H_2 with respective densities and velocities ρ_1, U_1 and ρ_2, U_2 (left panel of Fig. 11-1). If the lower layer is three times as thick as the upper layer and the lower layer is stagnant, what is the minimum value of the upper-layer velocity for which there is sufficient available kinetic energy for complete mixing (right panel of Fig. 11-1)?

11-2. In the ocean, a warm current ($T = 18°C$) flows with a velocity of 10 cm/s above a stagnant colder layer ($T = 10°C$). Both layers have identical salinities, and the thermal-expansion coefficient is taken as 2.54×10^{-4} K^{-1}. What is the wavelength of the longest unstable wave?

11-3. Formulate the Richardson number for a stratified shear flow with uniform stratification frequency N and linear velocity profile, varying from zero at the bottom to U at a height H. Then, relate the Richardson number to the Froude number and show that instabilities can occur only if the Froude number exceeds the value 2.

11-4. In an oceanic region far away from coasts and strong currents, the upper water column is stably stratified ($N = 0.015$ s^{-1}). A storm passes by and, during 10 h, exerts an average stress of 0.2 N/m^2. What is the depth of the mixed layer by the end of the storm? (For seawater, take $\rho_0 = 1028$ kg/m^3.)

11-5. An air mass blows over a cold ocean at a speed of 10 m/s and develops a stable potential-temperature gradient of 8°C per kilometer. It then encounters a warm continent

and is heated from below at the rate of 200 W/m^2. Assuming that the air mass maintains its speed, what is the height of the convective layer 60 km inshore? What is then a typical vertical velocity of convection? (Take $\rho_0 = 1.20$ kg/m^3, $\alpha = 3.5 \times 10^{-3}$ K^{-1}, and $C_p = 1005$ $J/kg \cdot K$.)

11-6. For the growing atmospheric boundary layer, show that thermals rise faster than the layer grows ($w_* > dh/dt$) and that thermals have a temperature contrast less than the temperature jump at the top of the layer [$T_* < (T - T_0)/2$].

SUGGESTED LABORATORY DEMONSTRATION

Equipment

A long, transparent container of rectangular cross-section, dyed sugar water, a continuous supply of fresh water.

Experiment

Divide the container into three sections by means of vertical, watertight partitions that do not extend to the top of the tank (in order to allow overflow from one section to the next). Arrange these partitions to create two short end sections and one long middle section. Fill the middle section to the brim with dyed sugar water. With a faucet and hose, supply fresh water at a constant rate to one of the end sections, and let it spill over the middle section, mix with the sugar water, and empty into the third section. Observe the entrainment of dyed water in the upper flow and the concomitant penetration of mixing. Watch for a wave on the interface traveling upstream from the second partition. (Adapted from Ellison and Turner, 1959.)

Lewis Fry Richardson

1881 – 1953

Unlike many scientists of his generation and the next, Lewis Fry Richardson did not become interested in meteorology because of a war. On the contrary, he left his secure appointment at the Meteorological Office in England during World War I to serve in a French ambulance convoy and tend the wounded. After the war, he returned to the Meteorological Office, only to leave it again when it was transferred to the Air Ministry, deeply convinced that "science ought to be subordinate to morals". Richardson's scientific contributions span finite-difference solutions of differential equations, meteorology, and mathematical modeling of nations at war and in peace. The marriage of his first two interests led him to conceive of numerical weather forecasting well before computers were available for the task. His formulation of the ratio that now bears his name is found in a series of landmark publications in 1919–1920 on atmospheric turbulence and diffusion. According to his contemporaries, Richardson was a clear thinker and lecturer, with no enthusiasm for administrative work and a preference for solitude. He confessed to being "a bad listener because I am distracted by thoughts." (*Photo credit: Bassano and Vandyk, London.*)